Supporting Assessment of Forest Burned Areas by Aerial Photogrammetry: The Susa Valley (NW Italy) Fires of Autumn 2017

S. De Petris, E. J. Momo, and E. Borgogno-Mondino(✉)

DISAFA, University of Torino, L.go Braccini 2, 10095 Grugliasco, TO, Italy
enrico.borgogno@unito.it

Abstract. In October 2017, a large wildfire occurred in the Susa valley (Italian Western Alps) affecting wide areas of mixed forests (*Pinus sylvetris* L.; *Fagus sylvatica* L., *Quercus pubescens* Willd.) with a spot pattern. Few days after the event an aerial survey operated by an RGB camera Sony ILCE-7RM2-a7R II was done with the aim of testing a digital photogrammetry-based 3D rapid mapping of fire effects. Flight altitude was about 800 m above ground level (AGL) determining an average image GSD of about 0.2 m. Image block adjustment was performed in *Agisoft PhotoScan vs 1.2.4* using 18 ground control points that were recognized over true color orthoimages (GSD = 0.4 m). Height values of GCPs were obtained from a 5 m grid size DTM. Both orthoimages and DTM were obtained for free from the Piemonte Region Cartographic Office (ICE dataset 2010). A point cloud, having an average density of 7 pt/m^2 and covering 14 km^2 was generated, filtered and regularized to generate the correspondent DSM (Digital Surface Model) with a grid size of 0.5 m. With reference to the above-mentioned ICE DTM, a Canopy Height Model (CHM) was generated by grid differencing with a grid size of 0.5 m. A true-orthoimage was also generated having a GSD of 0.5 m. The latter was used to map burned areas by a pixel based unsupervised classification approach operating with reference to the pseudo GNDVI image, previously computed from the native red and green bands (no radiometric calibration was applied aimed at converting back the raw digital numbers to reflectance). Results were compared with 2 official datasets that were generated after the event from satellite data, one produced by the Piemonte Region and the other one by the Copernicus Emergency System. In order to test differences between burned and not-burned areas, point density, point spacing and canopy heights were computed and compared looking for evidences of geometrical differences possibly characterizing burned areas in respect of the not burned ones. Results showed that no significant differences were found between point density and point spacing in burned and not burned area. There was a significant difference in CHM minimum values distribution between burned and not-burned areas while maximum values distribution does not change significantly, proving that fire change crown structure but tree height remain unchanged. These results suggest that aerial photogrammetry could detect fire effect on forest having higher accuracy respect to ordinary approaches used in forest disturbance ecology.

Keywords: Forest fire · Photogrammetry · Forest structure

© Springer Nature Switzerland AG 2020
O. Gervasi et al. (Eds.): ICCSA 2020, LNCS 12252, pp. 829–844, 2020.
https://doi.org/10.1007/978-3-030-58811-3_59

1 Introduction

In case of forest fire, mapping and characterization of those areas that have changed has great importance for future planning and decision making. Geomatics techniques are essential for forest fire monitoring, especially in region characterized by difficult accessibility and large surfaces; they are widely used to map burned and unburned areas measuring fire severity, i.e. environmental change caused by fire and corresponding to the loss or decomposition of below- and above-ground biomass. The knowledge of temporal and spatial patterns of severity is essential to assess the ecological effects of recent fires. The creation of fire severity maps gives a valuable tool to support post-fire management and/or evaluate the success of fuel treatments [1]. In this context many approaches based on remotely sensed data are used supporting many operative protocols in response to forest fire [2, 3]. Spectral vegetation indices from optical data are used to monitor vegetation changes after fire [4]; other indices like Normalized Burn Ratio (NBR), differenced NBR (dNBR), relative dNBR (RdNBR) and MIRBI were proposed to specifically map burned and unburned areas aiming at measuring fire severity [5]. Optical remotely sensed data are widely used coupling easy accessibility and interpretability with reasonably accurate estimates of burn severity [5]. Nevertheless, spatial resolution and monoscopy of these data limit ecological description of fire effects, making them unable to describe local variations at a higher spatial scale [6]. LiDAR (Light Detection and Ranging, [7, 8]) is known to be able to, conversely, provide three-dimensional measures that can be used to estimate forest parameters as tree height, leaf area index (LAI) and above ground biomass, needed for describing forest structure and monitoring structural changes [9]. A main advantage of LiDAR technique is the capability of generating detailed DTMs (Digital Terrain Models) under forest canopy, fundamental step to normalize an image-based or point cloud respect to ground level. Nevertheless, in recent years, digital photogrammetry has been proposed as a possible alternative to LiDAR. Some studies [10] showed that photogrammetry is capable of mapping forest structure with an accuracy similar to LiDAR, but at lower cost; current image matching algorithms allow to generate point clouds with a higher density than LiDAR making possible to accurately estimate forest metrics, e.g. tree height, stem volume, basal area and biomass [11]. Consequently, photogrammetry represents an important opportunity to monitor fire severity and fire effects on forestry stands giving, possibly, estimates of stem volume lost. In this work a test concerning exploration of digital photogrammetry potentialities in mapping fire effects is presented, based on data obtained by an aerial survey operated by an RGB camera in the Susa Valley (Italian Western Alps) after a large wildfire event occurred in October 2017. In particular, authors focused on the following issues: (a) classification of burned areas; (b) characterization of burned and not-burned areas testing differences of point cloud features (point density, point spacing and canopy heights); (c) estimation of wood volume damaged/burnt by fire.

2 Materials and Methods

2.1 Study Area

The study area (AOI - Area Of Interest) is located in the municipalities of Bussoleno and Mompantero in Susa Valley (Italian Western Alps), being part of a wider area interested by a great wildfire in October 2017. AOI show a dominant south slope aspect and extends for about 14 km^2 covering a range of altitude from 450 m to 1500 m above sea level. In the area, about 920 ha are covered by forests dominated by different species such as scots pine (23% of surface), beech (15%) and other broadleaves (62%) like downy oak, chestnut, maple, ash and linden. Climatic conditions of this area are peculiar for Alps, being characterized by low annual rainfall, frequent wind and temperature rarely lower than 0 °C. October 2017 was characterized by anomalous weather conditions where high temperature and a prolonged lack of rainfall became the predisposing factors for wildfires that, in the same period, interested a lot of forests in the whole Piemonte Region. A large wildfire occurred finally in AOI in the second part of October. According to the post-fire assessment operated by the Piemonte Region [12], about 50% of the area interested by fire was characterized by a medium or high fire severity, especially in stands dominated by scots pine, beech, and, secondly, by larch and chestnut. Some beech stands were also interested by a wildfire in 2003 making them particularly critical [13] (Fig. 1).

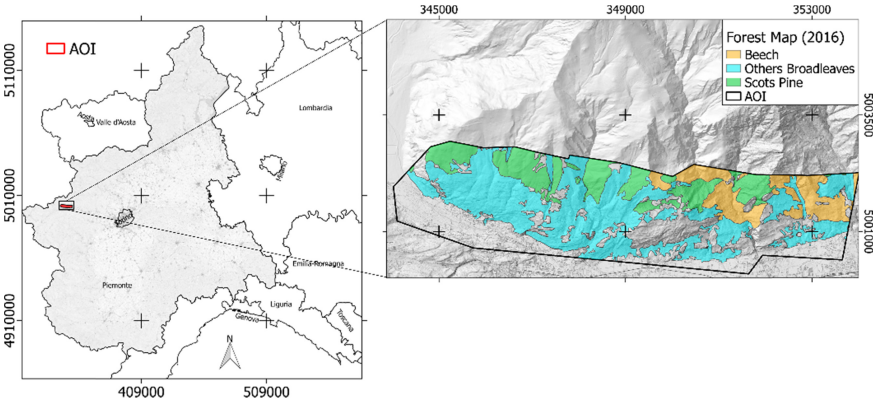


Fig. 1. (Left) Study area is located in mesalpic zone of Susa valley, Piemonte region (NW – Italy). (Right) Main forest types present in the area (Reference frame: WGS84 UTM32N).

2.2 Photogrammetric Workflow

The photogrammetric aerial survey was operated on 10th November 2017 (few days after fire stopped) by DIGISKY s.r.l. company. During the flight a Tecnam P92 JS airplane was used equipped with SmartBay©, a device for boarding up to three different sensors simultaneously on the wing lower surface (intrados) in order to quickly and efficiently reconfigure the payload and to perform complex, aerial mapping

missions. SmartBay© is equipped with its own mission computer that automatically manages all remote sensing activities (Payload Control System) during the mission while providing the pilot with all needed to conduct the aircraft (Crew Operator Deck). An RGB camera Sony ILCE-7RM2-a7R II, focal length = 28 mm, CMOS full frame 42 MP, pixel size = 4.53 μm was used. Flight direction was parallel to valley and flying altitude above ground level (AGL) ranged between 500–1200 m, determining an average baseline of about 43 m. Three-hundred-one images (13 Mb per image) were acquired with GSD (Ground Sample Distance) sizing between 0.05–0.2 m. Forward overlap ranged between 90 and 97%, side overlap between 85 and 96%. Image block was processed by *Agisoft Photoscan vs 1.2.4*. Eighteen ground control points (GCPs) were collected after the flight (Fig. 2) by photointerpretation from the available AGEA True-color orthophotos (2015) having a GSD = 0.5 m. Height value was obtained from the gridded Piemonte-ICE Digital Terrain Model (DTM), having a grid size of 5 m and a height precision of 0.6 m (σ_z). After image block bundle adjustment, a dense point cloud (PPC) was generated. PPC was filtered and regularized using *LAStools* [14] in order to create a Digital Surface Model (DSM) with a grid size of 0.5 m. Finally, a true color ortho-mosaic (TCOM) having a GSD of 0.2 m (corresponding to a nominal map scale of 1:1000) was generated for the whole area.

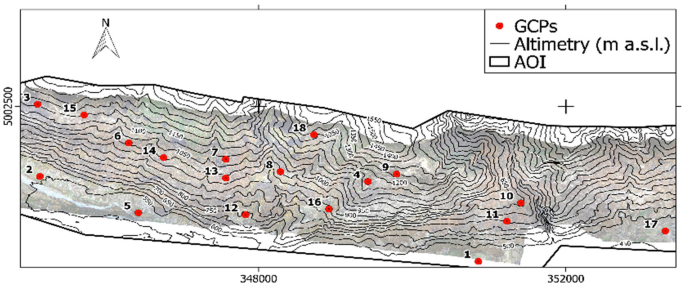


Fig. 2. GCPs location in the AOI with contour lines (Reference frame: WGS84 UTM32N).

2.3 Burned Area Detection

Available institutional Forest Map (FM) was obtained in vector format from the Piemonte region geoportal having a nominal scale 1:10000 (updated in 2016) mapping local forest types. With respect to FM all data from the photogrammetric process were masked in order to address following operation only onto forested area. From TCOM a green normalized difference vegetation index (GNDVI) was calculated according to (1) from RGB bands to minimize shadows effects across the scene. No radiometric calibration was applied to TCOM aimed at converting back the raw digital numbers to reflectance.

$$GNDVI = \frac{DN_{Green} - DN_{Red}}{DN_{Green} + DN_{Red}} \quad (1)$$

K-means unsupervised classification with 2 clusters was applied to GNDVI map in order to detect burned (B) or not-burned (NB) forest areas. The resulting two-class map (B-NB map) was vectorized. In order to assign the right meaning to the generated clusters, the Cumulated Frequency Distribution (CFD) of GNDVI map was generated at cluster level. With respect to CFD (Fig. 3) a threshold was found to distinguish B from NB. It resulted to be located in correspondence of the CFD inflection point (second derivate equal to 0), where GNDVI value was 0. Consequently, all forested pixels with GNDVI < 0 where labeled as B, the others as NB.

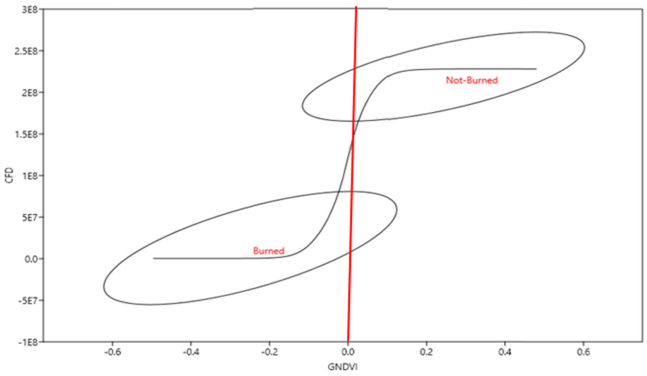


Fig. 3. CFD of GNDVI map. 95% Ellipses of two defined clusters. Redline shows the position of the selected threshold value (GNDVI = 0) used to classify B and NB forested areas. (Color figure online)

To explore the effects of fire on forest structure, two areas (burned and not burned crown, hereinafter called BC and NBC, respectively) sizing about 3.5 ha each and located over the same mountain slope were recognized on TCOM by photointerpretation (Fig. 4). According to FM, the same forest types and density were present in these areas. PPC points belonging to these areas were compared with the available DTM by differencing thus obtaining the correspondent NH value (Normalized Height, i.e. height from the ground level). Since NH values within the selected BC/NBC polygons were not normally distributed, the two statistical distribution were compared using the Kolmogorov-Smirnov non-parametric test and Mann-Whitney for equal median test. Other statistic moments like mean, median and quantiles were calculated, as well.

2.4 Damaged Trees Assessment

Photogrammetry already proved to be well performing in forest applications especially for tree counting and tree height measurement [15]. The joint use of both radiometric and geometric discriminants, possibly derived from photogrammetric survey can certainly improve tree state assessment after forest disturbance, e.g. wildfire and windstorm [16, 17]. Ordinarily, the adopted approach to derive forest parameters is based on

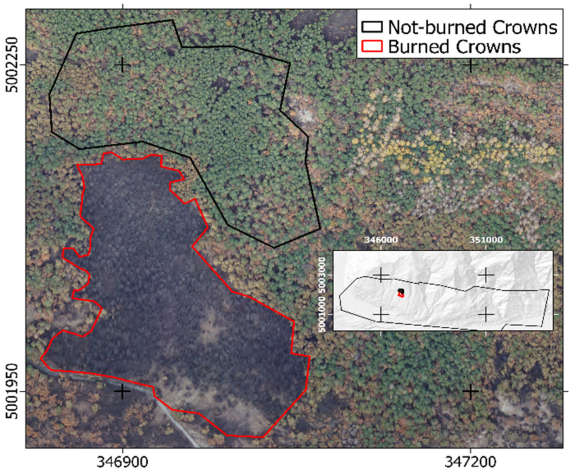


Fig. 4. Polygons show the two selected areas representing burned (BC, Red) and not burned (NBC, Black) crowns. They size approximately 3.5 ha each. According to FM the main forest type in the area is Scots Pine and tree density is similar (Reference frame: WGS84 UTM32N). (Color figure online)

Canopy Height Models (CHM) processing [15]. Consequently, in this study, a CHM was calculated by grid difference between DSM and DTM, covering the whole AOI. Tree counting (Tree Tops –TT) was performed using the Local Maxima (LM) approach operating over the CHM. This algorithm finds tree highest apex within a given crown that were assumed as representative of a single tree position. In particular, CHM analysis was performed by the Forest Tools [18] developed by using R programming language working with a Variable Window Filter algorithm (VWF); VWF is a local maxima operator [19] that changes its size according to a determinate function, that, for this work, was related to the local tree height (2). Local height values used to find the local maxima were recorded as attribute to the generated TT point vector layer. During the process points having a height local value lower than 3 m were filtered out.

$$VWF\ size = DN_{CHM}\, 0.05 + 0.6 \tag{2}$$

An estimate of trees stem volume within the areas damaged by fire was computed using tree height information from TT, an hypsometric curve provided by the Territorial Forestry Planning – PFT [20] and the volume equation obtained from Tabacchi and his collaborators [21]. For each of the main local species (scots pine, beech and other broadleaves) a dendrometric function was calibrated, relating tree height with stem volume (Fig. 5). Once calibrated, functions were applied to all TT points to give an estimate of the amount of wood volume interested by fire.

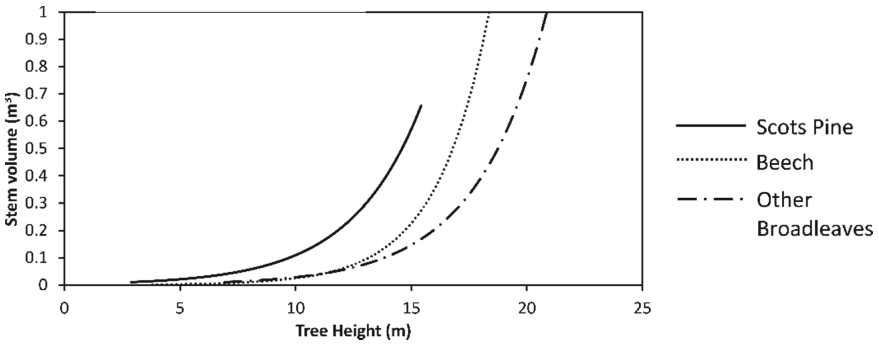


Fig. 5. Three dendrometric functions calibrated from PFT and Tabacchi [20, 21] showing relationship between single tree stem volume and tree height.

2.5 Reference Data

Burned Area

The Delineation Map (DM), nominal scale 1: 22,000, provided by Copernicus EMS – Mapping Service was obtained in vector format (Activation: EMSR253 – Susa). DM shows the fire delineation derived from post-event satellite image (Plèiades-1A/B) acquired on 30th October 2017 by photointerpretation. Piemonte Region institutional post-fire map (PFM) was also collected [12] in vector format (nominal scale 1:100,000). Metadata report that PFM was created with reference to FIREMON - Fire Effects Monitoring and Inventory System protocol [2] involving both optical remotely sensed (Sentinel-2 multispectral instrument) and ground-based data. DM and PFM (Fig. 6) were used as reference data to test relative accuracy of B-NB classes obtained by the authors.

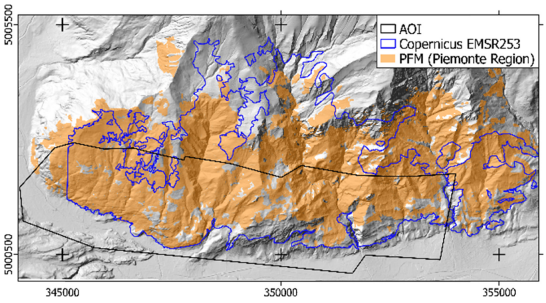


Fig. 6. Reference data used to compare classification results about B and NB areas. Black line (AOI) is the surveyed area by aerial (Reference frame: WGS84 UTM32N).

Tree Counting

Tree counting accuracy was tested by generating, randomly within burned areas, 50 virtual circular plots (VP) with 20 m radius. They were constrained to homogenously explore all the altitude zones. They sized about the 2% of total burned area. Ordinarily in forestry, tree density is estimated by counting all trees fallen in a given circular plot [22]; consequently, all crown centroids falling in each of the defined VP were counted by photo-interpretation of TCOM (Fig. 7). All trees lower than 3 m were filtered out in order to be consistent with the threshold previously defined.

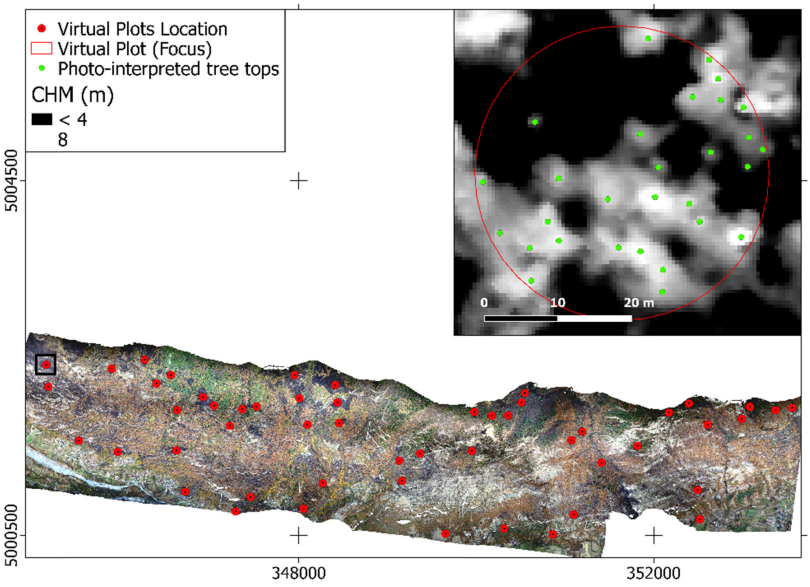


Fig. 7. VP distribution over burned area with a focus on example VP photo-interpretation procedure of tree tops (Reference frame: WGS84 UTM32N).

3 Results and Discussions

3.1 Image Bundle Adjustment and PPC

Bundle Adjustment was run using 18 GCPs having a 3D accuracy that can be estimated in 0.8 m (WGS84 UTM 32N). Accuracy of photogrammetric resection from the oriented image block showed the following values: σ_x = 0.63 m; σ_y = 1.33 m; σ_z = 1.74 m; $\sigma_{x,y,z}$ = 2.28 m. The obtained dense PPC contained 94 million points resulting in a point density of about 7 pt/m^2, and an average spacing of 0.4 m. After filtering and regularization, the correspondent DSM was generated with a GSD of 0.5 m, assuming that it maintained the same Z accuracy as the one of the photogrammetric resections. TCOM was, therefore, generated with a GSD of 0.2 m assuming having same XY accuracy as the one of the photogrammetric resections. To

assess the effects of fire on forest structure NH point cloud of BC (containing about 230000 points) was compared with NH point cloud of NBC (about 220000 points). BC point density and point spacing were respectively 7.62 pt/m^2 and 0.34 m; NBC point density and point spacing were 7.21 pt/m^2 and 0.37 m. In spite of these very similar results, the Kolmogorov-Smirnov test proved that the statistical distribution functions of the two areas were significantly different ($D = 0.5$, $p < 0.001$); the Mann-Whitney test proved that the two median values were different too ($U = 23292$, $p < 0.001$). Figure 8 shows the distributions of the normalized height values in BC and NBC. It can be noted that both mean and median values of BC are lower than those of NBC, proving that when fire severity is high, photogrammetry can penetrate canopy and reach the ground. As far as higher NH values are concerned, it can be noted that fire does not change significantly tree height. If we consider the previously estimated tree height measure accuracy, 1.74 m, upper NH values of BC and NBC are substantially the same. These results suggest that: (a) points resection efficiency from the oriented image block does not significantly changes in BC and NBC areas, being point spacing and density very similar; (b) high severity of fire significantly changes forest structure, but, in the short term, it doesn't affect tree height of the dominant layer; (c) photogrammetry proved to be effective to explore forest structure and assess fire severity.

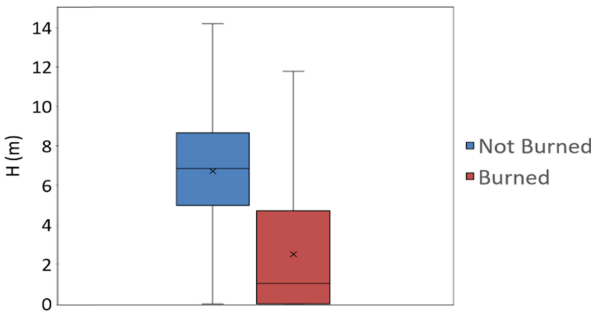


Fig. 8. CB-CNB NH distributions. Box-plot lines are respectively starting from bottom to up: minimum, Q1, median, Q3, x is mean value, maximum.

3.2 Burned Area Detection Accuracy

In Fig. 9 the produced B-NB map is reported. Statistics from classification are reported in Table 1 that shows that about 48% of the forested areas, about 447 ha, was classified as burned. Burned class equally affects main forest types in the area; in fact, about 50% of the area covered by each forest type proved to be damaged by fire (Table 1).

Classification accuracy was tested with respect to the available reference layers (DM and PFM). Classification accuracy is here defined as binary classification of imbalanced data since NB area was greater than B one [23]. Confusion matrix results and related accuracy measures are reported in Table 2. Precision and specificity were high (both 0.86) while balanced accuracy was 0.48 and 0.65 for DM and PFM respectively. Overall accuracy (defined as the ratio of correct decisions made by a

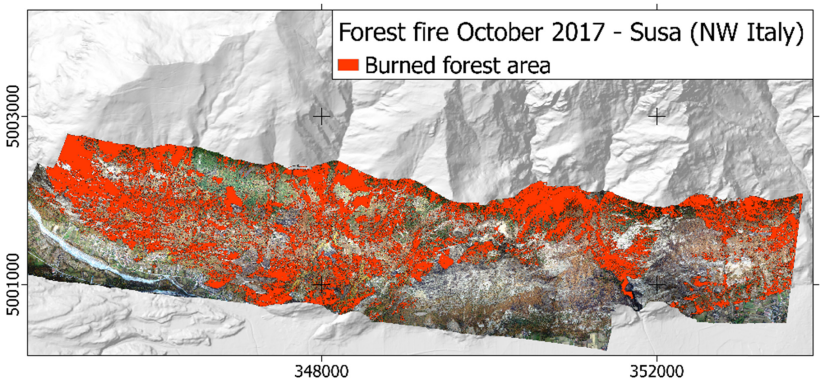


Fig. 9. B-NB map created by k-means unsupervised classification of GNDVI map (Reference frame: WGS84 UTM32N).

Table 1. Results of B-NB map reported by main forest types burned.

Forest type	Area (ha)	Burned area (ha)	Burned area (%)
Scots pine	218.18	111.04	50.89
Beech	136.14	67.41	49.52
Other broadleaves	566.81	268.68	47.40
Total	921.13	447.13	48.50

classifier) seem to be low: 0.57 and 0.47 for DM and PFM respectively, while F1 Score (harmonic mean of the precision and recall) and G-mean (geometric mean of sensitivity and precision) were high both in DM and PFM (about 0.6). These results suggest that classification of burned area based on K-means of high resolution GNDVI map is an effective approach. Regarding low overall accuracy is needed take in to account how reference data were generated.

DM was a product of rapid mapping procedure [24] therefore, since it was generated from high resolution satellite images, it suffers from the fast photointerpretation at small nominal scale (1:22000) compromising the delineation of medium/small or articulated areas. Furthermore, DM was not refined with any available forest map.

As far as PFM is concerned, it was the result of FIREMON-based protocol [12] which involved ground-based and remotely sensed data [25]. In particular, CBI - Composite Burn Index [26] was measured on ground-based plots while Sentinel-2 derived RdNBR was calculated as difference between images pre and post event and finally correlated with ground data to better calibrate a model to infer fire severity over large area. This procedure has problems related to fire severity model calibration. In fact, CBI summarizes both herbaceous/shrubs layer and tree canopy severity but, in closed forest canopy, remotely sensed data detect mainly the upper layer spectral response. Therefore, is very difficult inferring about dominated forest layers, making the calibration procedure heavily affected by this problem. Understory burns are

Table 2. Metrics derived from the confusion matrices of DM e PFM. TP (true positives): number of positive elements predicted as positive; FP (false positives): number of negative elements predicted as positive; FN (false negatives): number of positive elements predicted as negative; TN (true negatives): number of negative elements predicted as negative.

Measure	DM	PFM	Formula
Sensitivity	0.44	0.46	TPR = TP/(TP + FN)
Specificity (Producer's Accuracy)	0.86	0.50	SPC = TN/(FP + TN)
Precision (User's Accuracy)	0.86	0.83	PPV = TP/(TP + FP)
Negative Predictive Value	0.43	0.15	NPV = TN/(TN + FN)
False Positive Rate	0.14	0.50	FPR = FP/(FP + TN)
False Discovery Rate	0.13	0.17	FDR = FP/(FP + TP)
False Negative Rate	0.56	0.53	FNR = FN/(FN + TP)
Overall Accuracy	0.57	0.47	ACC = (TP + TN)/(P + N)
Balanced Accuracy	0.48	0.65	BA = TPR + TNR/2
F1 Score	0.58	0.60	F1 = 2TP/(2TP + FP + FN)
G-mean	0.62	0.61	G-mean = sqrt(TPR * PPV)

difficult to detect from satellite imagery due to interception of radiation and presence of shadows by the overstory layer especially where dense tree cover increases leaf area index (LAI) [27, 28]. Nevertheless, PFM constituted a real tool to better create priority zones where addressing restoration operations. All these considerations make clear that authors' intention was not having an absolute error estimate of their B-NB map, but comparing it with available data and measure relative correspondences.

3.3 Damaged Trees Counting Accuracy

A CHM of the area was obtained by grid differencing of DSM (from PPC) and DTM (from the Piemonte Region Geoportal). With reference to DSM and DTM height accuracies (1.74 m and 0.60 m respectively) and applying the variance propagation law CHM accuracy was found to be equal to 1.8 m. This result was similar to the one that can be obtained by ordinary forest ground-based tree height survey operated by hypsometer [29]. Starting from CHM, the TT vector layer was generated by LM approach. According to B-NB map, burned areas were considered where, reasonably, fire caused damages on trees. It is worth to remind that tree could be damaged on its trunk, the so called "*cat face*" [30], or on its crown [31]. Nevertheless, fire severity could change according to micro-station conditions [32]. Both these damages influence timber quality [33] and tree mortality [34]. Therefore, all detected trees in burned areas were considered as damaged and the corresponding biomass estimate computed (Fig. 10). Stem volume was estimated for each tree as recognized by the LM algorithm applying the correspondent dendrometric model. Results showed that about 26000 m^3 of stem biomass were damaged by the fire, distributed in the different forest type as reported in Table 3. It is possible to observe that, even though areas covered by scots pine is smaller than the one covered by broadleaves, the majority of wood volume interested by fire belong to this category.

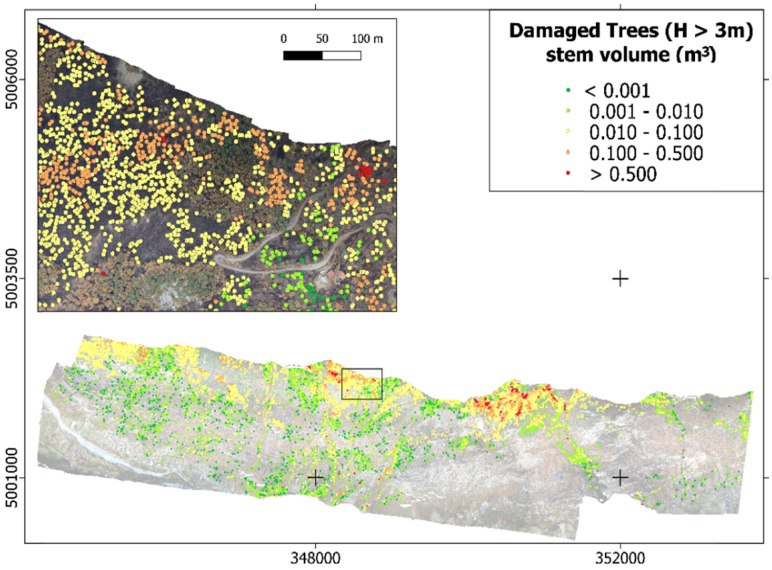


Fig. 10. Damaged trees (>3 m) as detected from the generated high-resolution CHM (Reference frame: WGS84 UTM32N). TT stems volume (m^3) are represented by a color code (see legend). A focus subset is reported too, showing that B-NB map combined with TT permits to separate burned crown trees (high severity) from the other ones (low severity/not burned).

Table 3. Distribution of wood damaged by forest type.

Forest type	V (m^3)	%
Scots pine	12153	46.82
Beech	2863	11.03
Other broadleaves	10937	42.14
Total	25953	

TT counting accuracy was tested with respect to tree density measured on 50 VP. A MAPE (Mean Absolute Percentage Error) equal to 30% was found proving that TT underestimated tree density. Similar results were reported by several studies [35, 36]. In particular, Pont [37] highlighted limitations of tree counting based on photo-interpretation. Nevertheless, photointerpretation of tree crowns by aerial images represents a reliable and cheaper [38] support when no ground data are available or surveyed areas are big and moving means large distances and, possibly, environmentally asper situations [39].

4 Conclusions

Susa forest fire of October 2017 was a relevant event that changed landscape and caused economic value loss of damaged trees. In general, after a fire, interactions with other natural hazards, e.g., debris flow and avalanches may delay forest regrowth and related restoring of ecosystem services [40]. Therefore, assessing and mapping fire effects is crucial to understand disturbance dynamics and to address interventions according to reliable criterion based on occurred changes. In this work authors have proposed a new approach based on low cost aerial photogrammetry (the cost can be estimated in about 2.5 euros/ha), that can be thought as alternative to a more traditional one based on satellite remote sensing or LiDAR acquisitions. Low cost aerial photogrammetry proved to be able to generated PPC, DSM and TCOM with a very high geometrical resolution and an accuracy that is comparable with the one affecting ordinary ground-based survey of forest parameters. A K-means based clustering of the obtained GNDVI map was run to classify burnt and not-burnt areas. The former, it was found, that covered about 447 ha in the area. Correspondent confusion matrix, generated after cluster interpretation and comparison with reference data, proved that this approach can be retained effective and classification accuracy (precision = 0.8) comparable with the one reported in other works about the same topic [41, 42]. A second goal of this study was to investigate effects of fire on forest structure. The comparison between NH values statistical distributions derived from PPC in B and NB areas, respectively, showed that in the short term, fire significantly changes crown structure (discovering the understory layers), but not tree height distribution in the dominant layer. Tree tops were mapped by LM showing an underestimation of about 30% of trees if compared with VP photointerpretation approach. In future it is expected that accuracy test could be referred to ground data. Detected TT were finally used to give an estimate of potentially damaged stem volume. This was achieved by applying proper dendrometric functions for the main local tree species. Potentially damaged stem volume was estimated to be approximately 26000 m^3. Finally, it can be said that the present study establishes a quantitative framework for detecting and measuring fire effects on forest structure. Future works will concern fire severity assessment through PPC local properties investigation. Unfortunately, this study did not cover the whole burned area in the Susa valley (about 2522 ha), limiting results to about the half of the area, according to the availability of aerial images. It is worth to remind that presented results cannot be completely generalized. In fact, for instance, no radiometric calibration was applied while generating TCOM. Moreover, classification of B and NB areas could fail if overstory layer shows a high LAI value or, conversely, low severity crown fire is present (mixed severity). Nevertheless, photogrammetry proved to be an effective technique to detect and characterize fire effects on forest with high geometrical resolution suggesting new research scenarios mainly related to single crown structure analysis.

Acknowledgments. We thank DIGISKY s.r.l (Strada Vicinale della Berlia, 500, 10146 Torino, Italy) for performing the aerial survey.

References

1. Arkin, J., Coops, N.C., Hermosilla, T., Daniels, L.D., Plowright, A.: Integrated fire severity–land cover mapping using very-high-spatial-resolution aerial imagery and point clouds. Int. J. Wildland Fire **28**(11), 840–860 (2019). https://doi.org/10.1071/WF19008
2. Lutes, D.C., et al.: FIREMON: fire effects monitoring and inventory system. Gen. Tech. Rep. RMRS-GTR-164. Fort Collins, CO: US Department of Agriculture, Forest Service, Rocky Mountain Research Station. 1 CD. 164 (2006)
3. De Santis, A., Chuvieco, E.: GeoCBI: a modified version of the Composite Burn Index for the initial assessment of the short-term burn severity from remotely sensed data. Remote Sens. Environ. **113**, 554–562 (2009)
4. Vo, V.D., Kinoshita, A.M.: Remote sensing of vegetation conditions after post-fire mulch treatments. J. Environ. Manage. **260**, 109993 (2020)
5. Furniss, T.J., Kane, V.R., Larson, A.J., Lutz, J.A.: Detecting tree mortality with Landsat-derived spectral indices: improving ecological accuracy by examining uncertainty. Remote Sens. Environ. **237**, 111497 (2020)
6. Hoe, M.S., Dunn, C.J., Temesgen, H.: Multitemporal LiDAR improves estimates of fire severity in forested landscapes. Int. J. Wildland Fire. **27**, 581–594 (2018)
7. Fissore, V., Mondino, E.B., Motta, R.: Limits and potentialities of gridded LiDAR data in the forest context: the case of the new Piemonte Region dataset. In: ForestSAT2014 Open Conference System, p. 1. AIT (2014)
8. Borgogno Mondino, E., Fissore, V., Falkowski, M.J., Palik, B.: How far can we trust forestry estimates from low-density LiDAR acquisitions? The Cutfoot Sioux experimental forest (MN, USA) case study. Int. J. Remote Sens. **41**, 4551–4569 (2020)
9. Su, Y., Guo, Q., Collins, B.M., Fry, D.L., Hu, T., Kelly, M.: Forest fuel treatment detection using multi-temporal airborne lidar data and high-resolution aerial imagery: a case study in the Sierra Nevada Mountains, California. Int. J. Remote Sens. **37**, 3322–3345 (2016)
10. Filippelli, S.K., Lefsky, M.A., Rocca, M.E.: Comparison and integration of lidar and photogrammetric point clouds for mapping pre-fire forest structure. Remote Sens. Environ. **224**, 154–166 (2019)
11. Bohlin, J., Wallerman, J., Fransson, J.E.: Forest variable estimation using photogrammetric matching of digital aerial images in combination with a high-resolution DEM. Scand. J. For. Res. **27**, 692–699 (2012)
12. Regione Piemonte: Piano straordinario di interventi di ripristino del territorio percorso dagli incendi boschivi dell'autunno 2017. (2019) https://www.regione.piemonte.it/web/sites/default/files/media/documenti/2019-04/Piano%20Straordinario%20interventi%20di%20ripristino.pdf
13. Ascoli, D., Castagneri, D., Valsecchi, C., Conedera, M., Bovio, G.: Post-fire restoration of beech stands in the Southern Alps by natural regeneration. Ecol. Eng. **54**, 210–217 (2013)
14. Isenburg, M.: LAStools-efficient tools for LiDAR processing (2012). http://www.cs.unc.edu/~isenburg/lastools/. Accessed 9 Oct 2012
15. Lisein, J., Pierrot-Deseilligny, M., Bonnet, S., Lejeune, P.: A photogrammetric workflow for the creation of a forest canopy height model from small unmanned aerial system imagery. Forests **4**, 922–944 (2013). https://doi.org/10.3390/f4040922
16. Chen, S., McDermid, G.J., Castilla, G., Linke, J.: Measuring vegetation height in linear disturbances in the boreal forest with UAV photogrammetry. Remote Sens. **9**, 1257 (2017)
17. Honkavaara, E., Litkey, P., Nurminen, K.: Automatic storm damage detection in forests using high-altitude photogrammetric imagery. Remote Sens. **5**, 1405–1424 (2013)

18. Plowright, A.: R package "ForestTools" (2018). https://github.com/andrew-plowright/ForestTools
19. Monnet, J.-M., Mermin, E., Chanussot, J., Berger, F.: Tree top detection using local maxima filtering: a parameter sensitivity analysis. In: 10th International Conference on LiDAR Applications for Assessing Forest Ecosystems (Silvilaser 2010) (2010). 9 p.
20. IPLA: PFT - Paini Forestali Territoriali, Regione Piemonte (2000)
21. Tabacchi, G., Di Cosmo, L., Gasparini, P.: Aboveground tree volume and phytomass prediction equations for forest species in Italy. Eur. J. Forest Res. **130**, 911–934 (2011). https://doi.org/10.1007/s10342-011-0481-9
22. van Laar, A., Akça, A.: Forest Mensuration. MAFE. Springer, Dordrecht (2007). https://doi.org/10.1007/978-1-4020-5991-9
23. Zliobaite, I.: On the relation between accuracy and fairness in binary classification. arXiv preprint arXiv:1505.05723 (2015)
24. Ajmar, A., Boccardo, P., Disabato, F., Giulio Tonolo, F.: Rapid Mapping: geomatics role and research opportunities. Rendiconti Lincei **26**(1), 63–73 (2015). https://doi.org/10.1007/s12210-015-0410-9
25. Morresi, D., Marzano, R., Motta, R., Garbarino, M.: Assessing fire severity through the integration of remote sensing and field burn indices: the big forest fires in North-Western Italy during autumn 2017. In: Geophysical Research Abstracts (2019)
26. Kasischke, E.S., Turetsky, M.R., Ottmar, R.D., French, N.H., Hoy, E.E., Kane, E.S.: Evaluation of the composite burn index for assessing fire severity in Alaskan black spruce forests. Int. J. Wildland Fire **17**, 515–526 (2008)
27. Cocke, A.E., Fulé, P.Z., Crouse, J.E.: Comparison of burn severity assessments using Differenced Normalized Burn Ratio and ground data. Int. J. Wildland Fire **14**, 189–198 (2005)
28. Rogan, J., Franklin, J.: Mapping wildfire burn severity in southern California forests and shrublands using Enhanced Thematic Mapper imagery. Geocarto Int. **16**, 91–106 (2001)
29. Bragg, D.C.: Accurately measuring the height of (real) forest trees. J. Forest. **112**, 51–54 (2014). https://doi.org/10.5849/jof.13-065
30. Norton, D.A.: Modern New Zealand tree-ring chronologies II: nothofagus menziesii. Tree-Ring Bull. (43), 39–49 (1983)
31. Weatherspoon, C.P., Skinner, C.N.: An assessment of factors associated with damage to tree crowns from the 1987 wildfires in northern California. For. Sci. **41**, 430–451 (1995)
32. Kane, V.R., et al.: Mixed severity fire effects within the Rim fire: relative importance of local climate, fire weather, topography, and forest structure. For. Ecol. Manage. **358**, 62–79 (2015)
33. Marschall, J.M., Guyette, R.P., Stambaugh, M.C., Stevenson, A.P.: Fire damage effects on red oak timber product value. For. Ecol. Manage. **320**, 182–189 (2014)
34. Catry, F.X., Rego, F., Moreira, F., Fernandes, P.M., Pausas, J.G.: Post-fire tree mortality in mixed forests of central Portugal. For. Ecol. Manage. **260**, 1184–1192 (2010)
35. Kattenborn, T., Sperlich, M., Bataua, K., Koch, B.: Automatic single tree detection in plantations using UAV-based photogrammetric point clouds. Int. Arch. Photogramm. Remote Sens. Spat. Inf. Sci. **40**, 139 (2014)
36. Nevalainen, O., et al.: Individual tree detection and classification with UAV-based photogrammetric point clouds and hyperspectral imaging. Remote Sens. **9**, 185 (2017)
37. Pont, D., Kimberley, M.O., Brownlie, R.K., Sabatia, C.O., Watt, M.S.: Calibrated tree counting on remotely sensed images of planted forests. Int. J. Remote Sens. **36**, 3819–3836 (2015)

38. Eid, T., Gobakken, T., Næsset, E.: Comparing stand inventories for large areas based on photo-interpretation and laser scanning by means of cost-plus-loss analyses. Scand. J. For. Res. **19**, 512–523 (2004)
39. Avery, T.E.: Forester's guide to aerial photo interpretation. US Department of Agriculture, Forest Service (1966)
40. Conedera, M., Peter, L., Marxer, P., Forster, F., Rickenmann, D., Re, L.: Consequences of forest fires on the hydrogeological response of mountain catchments: a case study of the Riale Buffaga, Ticino, Switzerland. Earth Surf. Proc. Land. J. Br. Geomorphol. Res. Group **28**, 117–129 (2003)
41. Wing, M.G., Burnett, J.D., Sessions, J.: Remote sensing and unmanned aerial system technology for monitoring and quantifying forest fire impacts. Int. J. Remote Sens. Appl. **4**, 18–35 (2014)
42. Cruz, H., Eckert, M., Meneses, J., Martínez, J.-F.: Efficient forest fire detection index for application in unmanned aerial systems (UASs). Sensors. **16**, 893 (2016)